Version 1.0 (June 22, 2007)
(Unpublished Manuscript: Do Not Cite or Quote Without Permission)

SELF-ORGANIZED CRITICALITY AND THE DEVELOPMENT OF EEG PHASE RESET

Thatcher, R.W. [1,2], North, D.M.[2], and Biver, C. J.[2]

Department of Neurology, University of South Florida College of Medicine, Tampa, Fl.[1] and EEG and NeuroImaging Laboratory, Applied Neuroscience, Inc., St. Petersburg, Fl[2]

Send Reprint Requests To:

Robert W. Thatcher, Ph.D.
NeuroImaging Laboratory
Applied Neuroscience, Inc.
St. Petersburg, Florida 33722
(727) 244-0240, rwthatcher@yahoo.com

ABSTRACT

Objectives: The purpose of this study was to explore human development of self-organized criticality (SOC) as measured by EEG phase reset from infancy to 16 years of age.

Methods: The electroencephalogram (EEG) was recorded from 19 scalp locations from 458 subjects ranging in age from 2 months to 16.44 years. Complex demodulation was used to compute instantaneous phase differences between pairs of electrodes and the 1st & 2nd derivatives were used to detect the sudden onset and offset times of a phase shift followed by an extended period of phase synchrony. Mean phase shift duration and phase synchrony intervals were computed for two symmetrical electrode arrays in the posterior-to-anterior locations and the anterior-to-posterior directions in the alpha frequency band (8 – 12 Hz).

Results: Log-log spectral plots demonstrated $1/f^{\alpha}$ distributions ($\alpha \approx 1$) with longer slopes during periods of "chaos" than during periods of phase synchrony. The mean duration of phase synchrony (150 – 450 msec) and phase shift (45 – 67 msec) generally increased as a function of age. The mean duration of phase shift declined over age in the local frontal regions but increased in distant electrode pairs. Oscillations and growth spurts from mean age 0.44 years to 16.22 years were consistently present.

Conclusions: The development of stability in local connections is paralleled by lengthened periods of "chaos" in distant connections. Development of the number and/or density of synaptic connections is a likely order parameter to explain oscillations and growth spurts in self-organized criticality during human brain maturation.

Key Words: Development of EEG phase reset, phase synchrony, chaos, self-organizational criticality.

1.0- Introduction

Understanding the mechanisms of neural synchronization and desynchronization is important in understanding human brain dynamics. Recent studies have shown that sudden transitions in the amplitude of the human electroencephalogram (EEG) are represented by power laws and scale invariance and long-range temporal correlations (Freeman 2003; Nikulin and Brismar, 2005; Linkenkaer-Hansen et al, 2001; Parish et al, 2004). These studies are important because long-range temporal correlations are a reliable method to transfer information in neuronal populations (Chialvo and Bak, 1999; Beggs and Plenz, 2003; Rios and Zang, 1999). The rapid creation and destruction of multistable spatiotemporal patterns have been evaluated in evoked, transient and spontaneous EEG studies (Breadspear and Terry, 2002a, 2002b; Rudrauf et al, 2006; Le Van Quyen, 2003). The patterns of spontaneously occurring synchronous activity involve the creation of temporary differentiated neural ensembles with oscillations and covarying phase at local, regional and large scales (Breakspear and Terry, 2002a; 2002b; Rudrauf et al, 2006; Stam and de Bruin, 2004; Varela, 1995; Freeman and Rogers, 2002). The dynamic balance between synchronization and desynchronization is considered essential for normal brain function and abnormal balance is often associated with pathological conditions such as epilepsy (Lopes da Silva and Pihn, 1995; LeVan Quyen et al, 2001b; Chevez et al, 2003; Netoff and Schiff, 2002). The integrated rapid sequencing of phase shifts followed by phase synchrony (i.e., the two fundamental components of phase reset) have been correlated to the alpha frequency band during cognitive tasks (Kahana; 2006; Kirschfeld, 2005; Tesche and Karhu, 2000; Jensen and Lisman, 1998),working memory (Rizzuto et al, 2003; Damasio, 1989; Tallon-Baudry et al, 2001), sensory-motor interactions (Vaadia et al, 1995; Roelfsema et al, 1997), hippocampal long-term potentiation (McCartney et al, 2004) and consciousness (Cosmelli et al, 2004; Varela et al, 2001; John, 2006). The present study builds on these previous studies by separately analyzing the two fundamental components of phase reset: 1- phase shift followed by, 2- phase stability.

Phase reset occurs in coupled nonlinear oscillators when there is a sudden shift of the phase relationship of oscillators to a new value followed by a period of phase locking or phase stability also called phase synchrony (Pikovsky et al, 2003). The term phase synchrony is synonymous with phase locking and is sometimes preferred in order to emphasize the statistical nature of phase stability (Rudrauf et al, 2006). Whether one refers to phase locking or phase synchrony what is important is the fact that there is a prolonged period of phase stability following a phase shift. This is important because

random phase shifts without stability exhibit "white noise" distributions (Pikovsky et al, 2003; Tass, 1997). Phase reset is also important because it results in increased EEG amplitudes due to increased phase synchrony of synaptic generators (Cooper et al, 1965; Nunez, 1994; Lopes da Silva, 1994). There are two general and equivalent methods for studying phase reset: 1- Short band decomposition and, 2- Broad band decomposition (Rudrauf et al, 2006; Le Van Quyen et al, 2001a). Both methods use analytic transforms such as the Wavelet transform and Hilbert transform. Which method is used depends on the frequency resolution desired and the nature of the transient signals that are to be detected (Rudrauf et al, 2006;Tass, 1997; Le Van Quyen et al, 2001a; Lachaux et al, 2000; Freeman et al, 2003; 2006; Freeman and Rogers, 2002). In the present paper we used a complex demodulation as an analytic signal processing method similar to that of Lachaux et al (2000) which is mathematically the same as the Hilbert transform (Pikovsky et al, 2003; Oppenheim and Schafer, 1975). All methods measure the temporal adjustment of pairs of signals evaluated over a successive frequency range or successive intervals of time with phase stability measured by the first derivative where phase stability is when the first derivative approximates zero or $d\varphi_{i,j}/dt \approx 0$. In general, the magnitude of phase shift is defined as the difference between the pre-phase shift value in degrees minus the post-phase shift value in degrees and if a sudden and significant phase difference occurs followed by an extended period of phase stability then the point in time when the phase shift occurred is the time when the first derivative was significantly positive and exceeded some threshold value (Rudrauf et al, 2006; Tass, 1997; Tass et al, 1998; Le Van Quyen et al, 2001a). This point in time marks the onset of phase reset. EEG phase shift offset is defined in a reverse manner and the onset and offset times define the phase shift duration. The phase shift duration is typically in the range of 10 msec to 80 msec (Buzaski, 2006; Freeman, 2003; Freeman and Rogers, 2002). Phase synchrony or phase stability that follows a phase shift is often 200 msec to 600 msec in duration in single cell analyses (Gray et al, 1989) and 100 msec to 1 second in surface recordings (Freeman and Baird; 1987; Freeman and Rogers, 2002; Freeman et al, 2006).

Recently, Linkenkaer-Hansen et al (2001); Stam and de Bruin (2004) and Freeman et al (2003; 2006) and Buzaski (2006) have shown that the EEG spectrum is best fit by a power function with a $1/f^{\alpha}$ distribution and that synchronization involves phase reset and self-organized criticality, where f = frequency and $\alpha \approx 1$. Self-organized criticality (SOC) is defined by brief periods approaching or reaching chaos followed by a period of phase stability and as mentioned previously are characterized by the invariant scaling properties of power laws and $1/f^{\alpha}$ (Bak et al, 1988). The analyses of Freeman et al (2003; 2006) demonstrated that the fine temporal structure of the EEG is characterized by repetitive

periods of "chaos" followed by a more extended period of "phase stability" and thus the human EEG fundamentally exhibits characteristics of "self-organizational criticality", where sudden phase shifts are "chaos" and phase locking is "phase stability" or "phase synchrony". Furthermore, these studies demonstrated that the terms "phase reset" and "SOC" are essentially synonymous in complicated systems (Bak et al, 1988; Bak, 1996; Rios and Zang, 1999).

Currently there are no studies of the early childhood development of EEG phase reset. Nikulin and Brismar (2005) studied EEG age dependence of $1/f^{\alpha}$ distributions in 96 adult subjects. Interesting age and gender correlations were presented, however, phase shift and phase stability were not separately analyzed. Developmental changes in the number of phase resets per second and the duration of phase shifts and the length of phase locking are currently unknown and such information may be important in understanding the development of human neural dynamics. Therefore, the purpose of the present study is to investigate the development of human EEG phase reset from infancy to 16 years of age. The null hypotheses to be tested in this study are: 1- there are no left and right hemispheric differences in the development of phase reset; 2- there are no differences in phase reset as a function of anterior-to-posterior vs. posterior-to-anterior direction, 3- there are no differences in phase reset as a function of inter-electrode distance and 4- there are no changes in phase reset as a function of age.

2.0 – Methods

2.1 Subjects

A total of 458 subjects ranging in age from 2 months to 16.44 years (males = 257) were included in this study. The subjects in the study were recruited using newspaper advertisements in rural and urban Maryland (Thatcher et al, 1987; 2003; 2007). The inclusion/exclusion criteria were no history of neurological disorders such as epilepsy, head injuries and reported normal development and successful school performance. None of the subjects had taken medication of any kind at least 24 hours before testing in this study. All of the school age children were within the normal range of intelligence as measured by the WISC-R and were performing at grade level in reading, spelling and arithmetic as measured by the WRAT and none were classified as learning disabled nor were any of the school aged children in special education classes. All subjects $\geq$ 1 years of age were given an eight-item "laterality" test consisting of three tasks to determine eye dominance, two tasks to determine foot dominance, and three tasks to determine hand dominance. Scores ranged from – 8 (representing strong sinistral preference or left handedness), to +8 (representing strong dextral preference or right handedness). Dextral

dominant children were defined as having a laterality score of ≥ 2 and sinistral dominant children were defined as having a laterality score of ≤ -2. Only 9% of the subjects had laterality scores ≤ 2 and 87% of the subjects had laterality scores ≥ 2 and thus the majority of subjects in this study were right side dominant.

2.2 EEG Recording

Power spectral analyses were performed on .58 to 2 minute 17 second segments of EEG recorded during an resting eyes closed condition. The EEG was recorded from 19 scalp locations based on the International 10/20 system of electrode placement, using linked ears as a reference. Eye movement electrodes were applied to monitor artifact and all EEG records were visually edited to remove any visible artifact. Each EEG record was plotted and visually examined and then edited to remove artifact using the Neuroguide software program (NeuroGuide, v2.3.8). Split-half reliability tests were conducted on the edited EEG segments and only records with > 90% reliability were entered into the spectral analyses. The amplifier bandwidths were nominally 0.5 to 30 Hz, the outputs being 3 db down at these frequencies. The EEG was digitized at 100 Hz and up-sampled to 128 Hz and then spectral analyzed using complex demodulation (Granger and Hatanaka, 1964; Otnes and Enochson, 1978) (see section 2.3).

EEG phase differences and phase reset metrics was computed in the alpha frequency band (8.0 – 12.5 Hz) for anterior-to-posterior electrodes Fp1/2-F3/4; Fp1/2-C3/4; Fp1/2-P3/4 and Fp1/2-O1/2 and for posterior-to-anterior electrodes O1/2-P3/4; O1/2-C3/4; O1/2-F3/4 and O1/2-Fp1/2. This recording arrangement provides a stable matrix and test of spatial homogeneity by using five equally spaced electrodes per hemisphere with increasing distance between electrodes in the anterior-to-posterior and posterior-to-anterior directions. According to volume conduction there is a homogeneous decline of voltage as a function of distance from any source at near zero phase delay. The five equally spaced electrode locations is a direct test of volume conduction versus cortical connectivity (Thatcher et al, 1986; 1998). Factors used in the multivariate analysis of variance were: 1- Hemisphere, 2- Direction, 3- Inter-electrode distance and 4- Age. The analyses of different frequency bands demonstrated that the alpha frequency band exhibits the strongest developmental trends and therefore this study will focus exclusively on the 8 – 12 Hz alpha frequency band (Niedermeyer and Lopes da Silva, 1994).

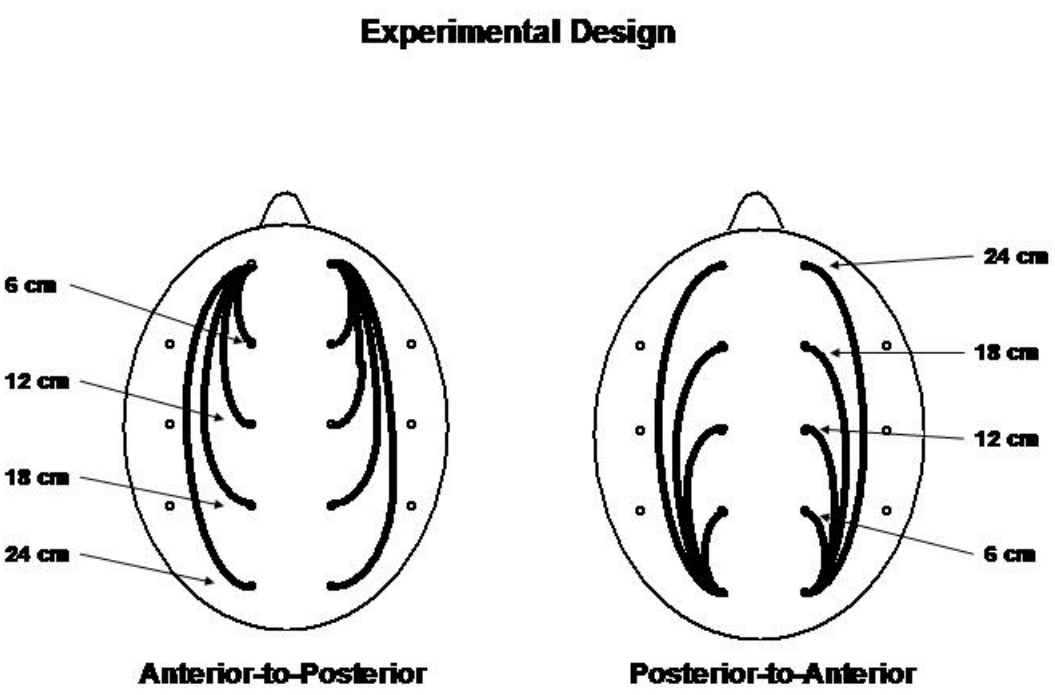

Fig. 1 – Experimental design. Left head diagram shows the location of electrodes for the computation of coherence and phase differences in the anterior-to-posterior direction. Right head diagram shows the location of electrodes in the posterior-to-anterior direction. Local distances (6 cm) are in adjacent electrode combinations (O1/2-P3/4 and Fp1/2-F3/4). Longest distance (24 cm) electrode combinations are Fp1/2-O1/2.

2.3 – Complex Demodulation and Joint-Time-Frequency-Analysis

Complex demodulation was used in a Joint-Time-Frequency-Analysis (JTFA) to compute instantaneous coherence and phase-differences (Granger and Hatanaka, 1964; Otnes and Enochson, 1978; Bloomfield, 2000). This method is an analytic linear shift-invariant transform that first multiplies a time series by the complex function of a sine and cosine at a specific center frequency (Center frequency = 10.0 Hz) followed by a low pass filter (6^{th} order low-pass Butterworth, bandwidth = 2.0 Hz) which removes all but very low frequencies (shifts frequency to 0) and transforms the time series into instantaneous amplitude and phase and an "instantaneous" spectrum (Bloomfield, 2000). We place quotations around the term "instantaneous" to emphasize that, similar to Hilbert transforms, there is always a trade-off between time resolution and frequency resolution. The broader the band width the higher the

time resolution but the lower the frequency resolution and vice versa. Mathematically, complex demodulation is defined as an analytic transform that involves the multiplication of a discrete time series $\{x_t, t = 1, \ldots, n\}$ by sine $\omega_0 t$ and cos $\omega_0 t$ followed by a low pass filter F,

$$Z'_t = F(x_t \sin \omega_0 t)$$

$$Z''_t = F(x_t \cos \omega_0 t)$$

and $2\left[(Z'_t)^2 + (Z''_t)^2\right]^{1/2}$ is an estimate of the instantaneous amplitude of the frequency ω_0 at time t and $\tan^{-1} \frac{Z'_t}{Z''_t}$ is an estimate of the instantaneous phase at time t. At this step the result of the complex demodulation transform is the same as the Hilbert transform (Pikovsky et al, 2003, p. 362).

The instantaneous cross-spectrum is computed when there are two time series $\{y_t, t = 1, \ldots, n\}$ and $\{y'_t, t = 1, \ldots, n\}$ and if F [ ] is a filter passing only frequencies near zero, then, as above

$R_t^2 = F[y_t \sin \omega_0 t]^2 + F[y_t \cos \omega_0 t]^2 = \left| F\left[y_t e^{i\omega_0 t}\right]^2 \right|$ is the estimate of the amplitude of frequency ω_0 at time t and

$\varphi_t = \tan^{-1}\left(\frac{F[y_t \sin \omega_0 t]}{F[y_t \cos \omega_0 t]}\right)$ is an estimate of the phase of frequency ω_0 at time t and since

$$F\left[y_t e^{i\omega_0 t}\right] = R_t e^{i\varphi_t},$$

and likewise,

$$F\left[y'_t e^{i\omega_0 t}\right] = R'_t e^{i\varphi_t}$$

the instantaneous cross-spectrum is

$$V_t = F\left[y_t e^{i\omega_0 t}\right] F\left[y'_t e^{-i\omega_0 t}\right]$$

$$= R_t R'_t e^{i[\varphi_t - \varphi'_t]}$$

and the instantaneous coherence is

$$\frac{|V_t|}{R_t^2 R_t'^2} \equiv 1$$

The instantaneous phase-difference is $\varphi_t - \varphi_t'$. That is, the instantaneous phase difference is computed by estimating the instantaneous phase for each time series separately and then taking the difference. Instantaneous phase difference is also the arctangent of the imaginary part of V_t divided by the real part (or the instantaneous quadspectrum divided by the instantaneous cospectrum) at each time point.

2.4 – Phase Straightening

Freeman et al (2006) used a method to "unwrap" phase to straighten the trigonometric actangent function. We used the phase "straightening" method of Otnes and Enochson (1978) achieve the same results. Both procedures are sufficient to solve the problem due to the phase angle intrinsic discontinuity, i.e., where 0 and 360 are at opposite ends while in the circular distribution $0^0 = 360^0$. The Otnes and Enochson (1978) procedure used in this study involves identifying the points in time when phase jumps from $+ 180^0$ to $- 180^0$ and then adding or subtracting 360^0 depending on the direction of sign change. For example, $\Delta\theta = (180 - \varepsilon)^0 + (180 - \varepsilon)^0 = 360^0 - 2\varepsilon$ which is the same as 2ε since $-(180 - \varepsilon)^0 = 180 + \varepsilon$. This procedure results in phase being a smooth function of time and removes the discontinuities due to the arctangent function. We found that absolute phase differences without phase straightening gave similar results to those presented in this study. This is because the vast majority of EEG phase relationships are less than $\pm 180^0$. However, phase straightening is important when computing the first and second derivatives of the time series of phase differences because the discontinuity between $- 180^0$ to $+ 180^0$ can produce artifacts. Accordingly, all of the derivatives and phase reset measures in this paper were computed after phase straightening.

2.5- Computation of the 1st and 2nd Derivatives of the Time Series of Phase Differences

The first derivative of the time series of phase-differences between all pair wise combinations of two channels was computed in order to detect advancements and reductions of phase-differences. The Savitzgy-Golay procedure was used to compute the first derivatives of the time series of instantaneous phase differences using a window length of 3 time points and the polynomial degree of 2 (Savitzgy-Golay, 1964; Press et al, 1994). The units of the 1st derivative are in degrees/point which was normalized to degrees per centisecond (i.e., degrees/cs = degrees/100 msec). The second derivative was computed using a window length of 5 time

points and a polynomial degree of 3 and the units are degrees per centiseconds squared (i.e., degrees/cs^2 = degrees/100 msec.^{2}).

2.6 – Calculation of Phase Reset

The time series of 1st derivatives of the phase difference from any pair of electrodes was first rectified by computing the absolute value of the 1st derivative (see fig. 2). The sign or direction of a phase shift is arbitrary since two oscillating events may "spontaneously" adjust phase with no known absolute zero starting point (Pikovsky et al, 2003: Tass, 2007). The onset of a phase shift was defined as a significant positive first derivative of the time series of phase differences between two channels, i.e., $d(\varphi_t - \varphi'_t)$ /dt > 0, criterion bounds = 5^0. Phase stability or phase synchrony is defined as that period of time after a phase shift where there is a stable near zero first derivative of the instantaneous phase differences or $d(\varphi_t - \varphi'_t)/dt \approx 0$. The criteria for a significant 1st derivative is important and in the present study a threshold criteria of 5^0 was selected because it was > 5 standard deviations of the mean and the mean magnitude of phase shift ranged from 25 deg/cs to 45 deg/cs. Changing the threshold to higher values was not significant, however, eliminating the threshold resulted in greater "noise" and therefore the criteria of 5^0 is a conservative criteria. Figure two illustrates the concept of phase reset. Phase differences over time on the unit circle are measured by the length of the unit vector r. Coherence is a measure of phase consistency or phase clustering on the unit circle as measured by the length of the unit vector r. The illustration in figure 2 shows that the resultant vector $r_1 = r_2$ and therefore coherence when averaged over time ≈ 1.0 even though there is a brief phase shift. As the number of phase shifts per unit time increases then coherence declines because coherence is directly related to the average amount of phase locking or phase synchrony (Bendat and Piersol, 1980).

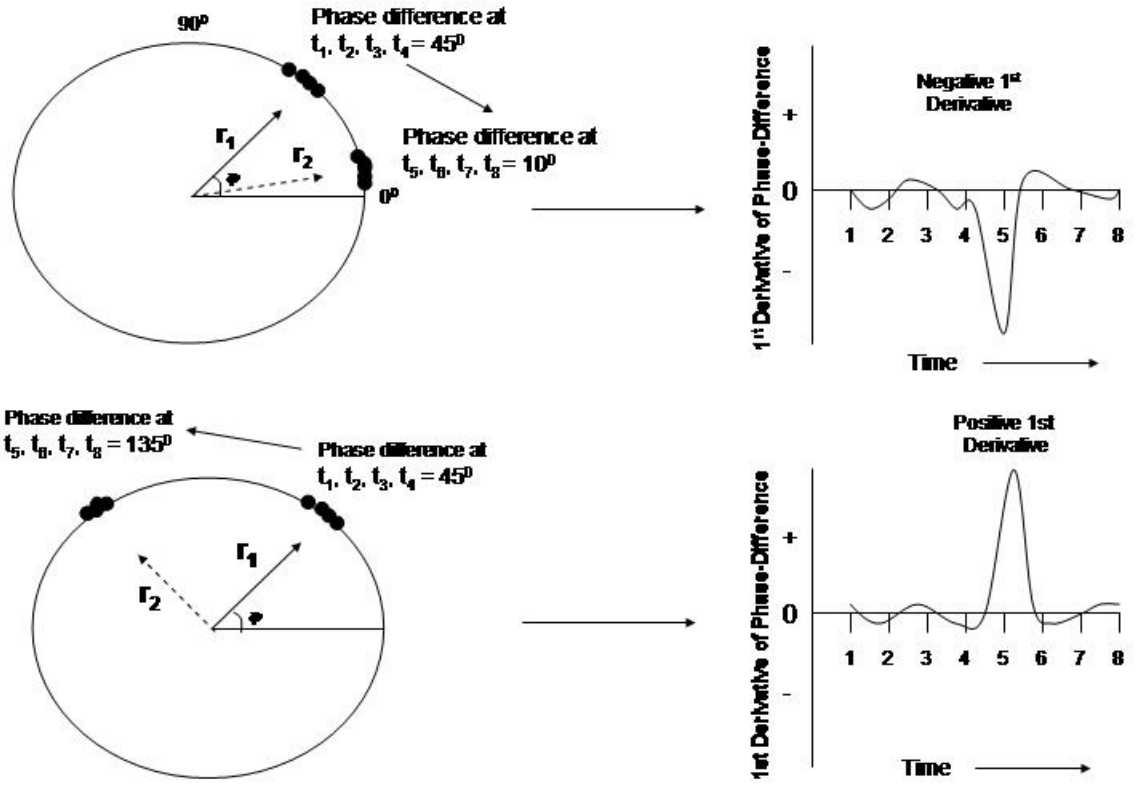

Fig. 2 – Illustrations of phase reset. Left is the unit circle in which there is a clustering of phase angles and thus high coherence as measured by the length of the unit vector r. The top row is an example of phase reduction and the top right is a time series of the approximated 1st derivative of the instantaneous phase differences for the time series t_1, t_2, t_3, t_4 at mean phase angle = 45^0 and t_5,t_6,t_7, t_8 at mean phase angle = 10^0. The vector r1 = 45^0 occurs first in time and the vector r2 = 10^0 and 135^0 (see bottom left) occurs later in time. Phase reset is defined by a sudden change in phase difference followed by a period of phase synchrony. The onset of Phase Reset is between time point 4 and 5 where the 1st derivative is a maximum. The 1st derivative near zero is when there is phase locking or phase synchrony and little change in phase difference over time. The bottom row is an example of phase advancement and the bottom right is the 1st derivative time series. The sign or direction of phase reset in a pair of EEG electrodes is arbitrary since there is no absolute "starting point" and phase shifts are often "spontaneous" and not driven by external events, i.e., self-organizing criticality. When the absolute 1st derivative ≈ 0 then two oscillating events are in phase synchrony and represent a stable state independent of the direction of phase shift.

Figure 3 shows the time markers and definitions used in this study. As mentioned above the peak of the absolute 1st derivative was used in the detection of the onset and offset of a phase shift and the second derivative was used to detect the inflection point which defines the full-width-half-maximum (FWHM) and phase shift duration. As seen in Figure 3, Phase Reset (PR)

is composed of two events: 1- a phase shift of a finite duration (SD) and 2, followed by an extended period of phase synchrony as measured by the phase synchrony interval (SI) and PR = SD + SI. Phase Shift duration (SD) is the interval of time from the onset of phase shift to the termination of phase shift where the termination is defined by two conditions: 1- a peak in the 1^{st} derivative (i.e., 1^{st} derivative = 0) followed by a succession of negative 1^{st} derivative values and, 2- a peak in the 2^{nd} derivative or inflection on the declining side of the time series of first derivatives. The peak of the 2^{nd} derivative marked the end of the phase shift period. Phase shift duration is the difference in time between phase shift onset and phase shift offset or $SD(t) = S(t)_{onset} - S(t)_{offset}$. Phase synchrony interval (SI) was defined as the interval of time between the end of a significant phase shift (i.e., peak of the 2^{nd} derivative) and the beginning of a subsequent significant phase shift (i.e., marked by the peak of the 2^{nd} derivative and the presence of a peak in the 1^{st} derivative) or $SI(t) = S(t)_{offset} - S(t)_{onset}$ See figure 3 diagram of phase shift duration and phase synchrony intervals. In summary, two measures of phase dynamics were computed in this study: 1- Phase shift duration (msec) (SD) and, 2- Phase synchrony interval (msec) (SI). The number of phase resets per second is a function of phase reset duration and phase synchrony or $PR/sec = (SD + SI)^{-1}$. Figure three illustrates the phase reset metrics and figure four shows an example of the computation of phase reset metrics in a single subject.

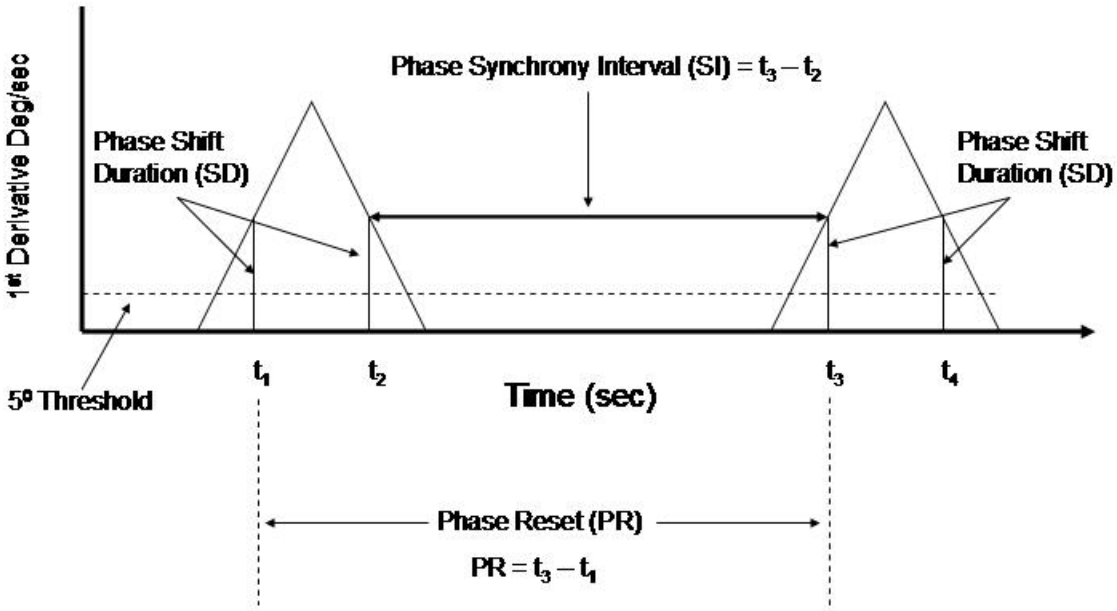

Fig. 3- Diagram of phase reset metrics. Phase shift (PS) onset was defined at the time point when a significant 1st derivative occurred ($\geq 5^0$ /centisecond), phase shift duration (SD) was defined as the time from onset to offset of the phase shift and the phase synchrony interval (SI) was defined as the interval of time between the onset of a phase shift and the onset of a subsequent phase shift. Phase reset (PR) is composed of two events: 1- a phase shift and 2- a period of synchrony following the phase shift where the 1st derivative ≈ 0 or PR = SD + SI.

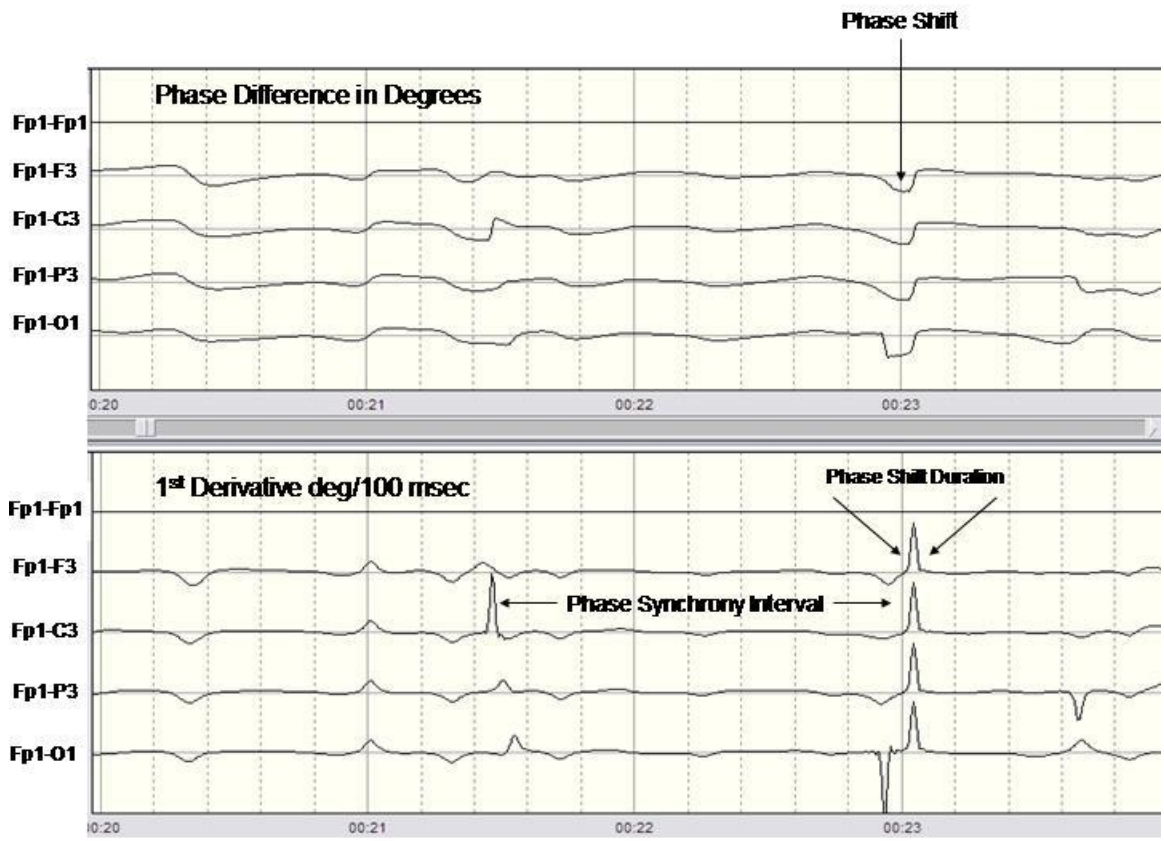

Fig. 4- Example from one subject. Top are the EEG phase differences between Fp1-F3, Fp1-C3, Fp1-P3 and Fp1-O1 in degrees. Bottom are the 1st derivatives of the phase differences in the top traces in degrees/centiseconds. A 1st derivative $\geq 5^0$ /cs marked the onset of a phase shift and an interval of time following the phase shift where the 1st derivative ≈ 0 defined the phase synchrony interval as described in figure 3.

2.7 – Sliding Averages

In order to increase temporal resolution one year sliding averages of EEG phase differences were computed. The procedure involved computing means and standard deviations for phase synchrony intervals and phase shift intervals over a one year period, e.g., birth to 1 year, then computing means and standard deviations from 0.25 years to 1.25 years, then a mean and standard deviation for the ages from 0.5 years to 1.5 years, etc. This resulted in a 75% overlap of subjects per mean with totally unique subjects on a one year interval. The sliding average procedure produced 64 equally spaced mean values with a 0.25 year resolution.

2.8 – Spectral Analyses of 1/f distribution

To evaluate possible 1/f spectral distributions the fast Fourier transform (FFT) of the time series of the 1st derivative of phase differences were computed for individual subjects using

edited EEG data. The FFT epoch length was 2 seconds and the sample rate was 128 Hz. Computations were first conducted on the entire edited EEG record (58 sec to 2 min 17 sec) and then separate selections of periods of phase shift and phase synchrony were subjected to separate FFT analyses in order to determine if the spectra were different between the phase synchrony vs. the phase shift periods in the EEG record. Tests of the 1/f distribution involved plotting the $\log_{10}$ transforms of frequency and magnitude and then a linear regression was used to determine the slope (α coefficient) and intercept of the linear fit.

2.9 – Spectral Analyses of Developmental Ultraslow Oscillations During the Lifespan

As explained in section 2.7, the sliding averages produced 64 equally spaced mean values of phase shift duration and phase synchrony intervals in each electrode pairing (at 3 month or 0.25 year resolution) from 0.44 years to 16.22 years. This resulted in a developmental time series of equally spaced mean ages for phase shift duration and phase synchrony intervals which were then spectrally analyzed. After detrending, the Fast Fourier Transform (FFT) was used to analyze the frequency spectrum of the developmental trajectories of phase shift and phase synchrony. The number of time points = 64, and the epoch length or Lifespan = 16.22 years. This produced a frequency resolution of 6 months and a maximum frequency of 32 cycles per epoch. The units of frequency were cycles per lifespan (cpl) and wavelength (λ) = 16.22/cpl. The units of frequency are cpl. The magnitude of the spectrum plotted on the y-axis are milliseconds/cycle/lifespan or msec/cpl.

3.0 – Results

3.1 – 1/f Phase Reset Distributions

As discussed in the introduction, the human EEG is often characterized by 1/f distributions which are revealed by log-log plots of the power spectrum (Freeman et al, 2003; 2006; Buzaki, 2006). All of the subjects in this study exhibited 1/f distributions of the 1st derivative of phase differences. Figure 5 shows examples of linear regression fits of the log-log plots of the

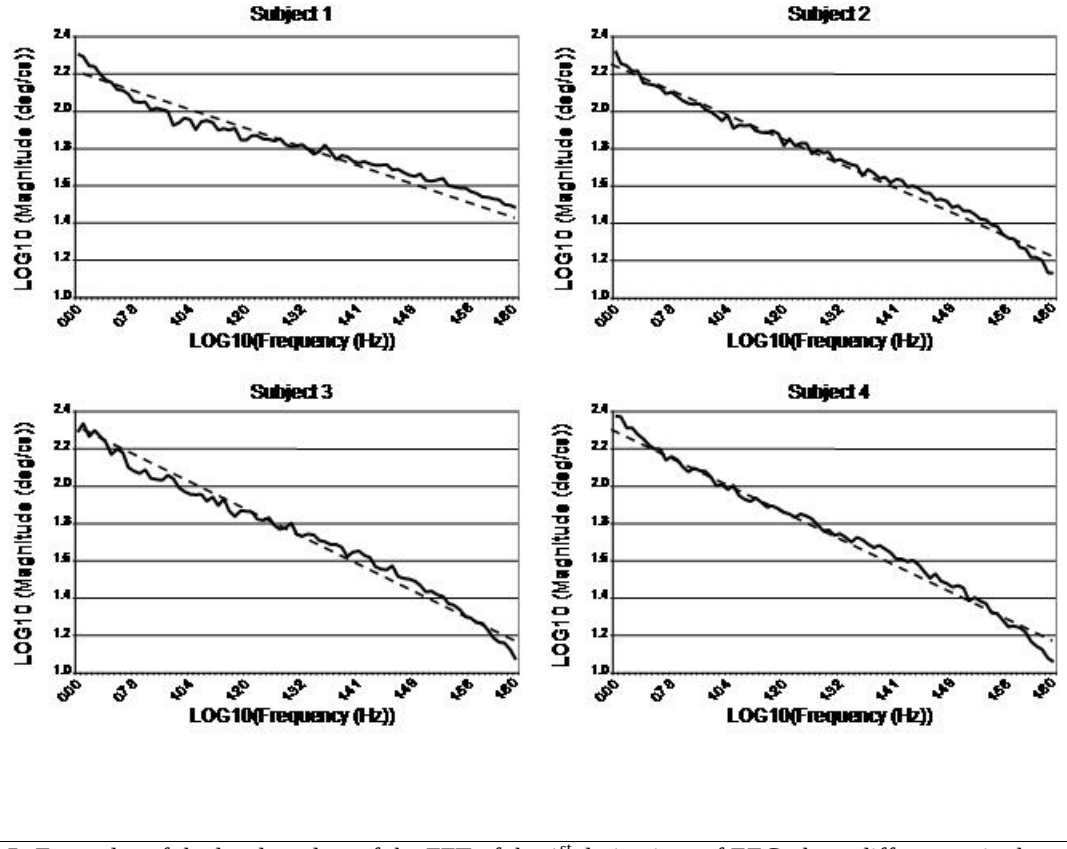

Fig. 5- Examples of the log-log plots of the FFT of the 1st derivatives of EEG phase differences in the anterior-to-posterior direction. Solid line is the FFT spectral values and the dotted line is the linear regression fits to the spectral values. Table I shows the slope or α exponents in the $1/f^{\alpha}$ equation.

power spectrum of the 1st derivative of phase differences in four subjects in the anterior-to-posterior direction. Very similar spectra were obtained independent of direction of hemisphere. Table I shows the slope or α values, the intercept and the regression correlation coefficients which all yielded $1/f^{\alpha}$ spectral distributions with a range from – 0.86 to – 0.54 and the average α = -0.76. To further investigate the nature of the 1/f distribution, sub-component analyses were conducted by selecting the 1st derivative of phase difference during phase reset by separately selecting the phase shift periods and phase synchrony periods and then spectrally analyzing the two different data selections. Frequency and magnitude were $\log_{10}$ transformed and linear regression fits were conducted in order to determine the slopes of the spectra. The results of the sub-component analyses are shown in figure 6 and Table II. As can be seen in figure 6 and Table II

Table I

Linear Regression Fit to the Log-Log of the FFT

REGRESSIONs	Subject 1	Subject 2	Subject 3	Subject 4
SLOPE - α	0.5419	0.7543	0.8066	0.8634
CORRELATION	0.966	0.917	0.914	0.918
SIGNIFICANT	P<.0001	P<.0001	P<.0001	P<.0001

Table I – The results of the linear regression fit to the log-log power spectra in Figure 5. The sign of the correlation and α is in accordance with $1/f^{\alpha}$.

In all instances and in all subjects the slope of the linear fit was > 1.0 for phase synchrony and < 1.0 for phase shift periods. The average slope or α coefficient was close to 1.0 with a mean = 1.0466. As seen in Table II, there were statistically significant differences in slope (i.e., α) between periods of phase shift vs. periods of phase synchrony where the slope was always steeper for phase synchrony than phase shift.

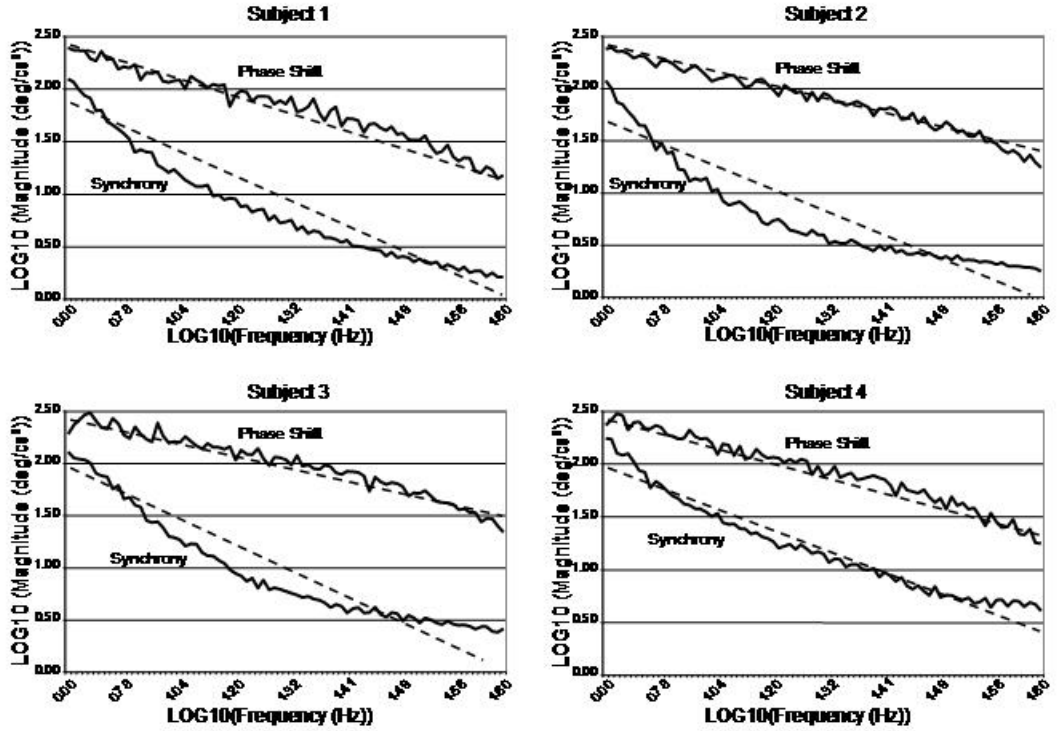

Fig. 6- Log-log plots of the Fourier analyses of the 1st derivative of phase differences during periods of phase synchrony versus periods of phase shift in the four different subjects in figure 5. Solid line is the FFT spectral values and the dotted line is the linear regression fits to the spectral values. A $1/f^{\alpha}$ distribution is present in all instances in which the slope coefficients were higher for the phase synchrony periods in comparison to the phase shift periods. Table II shows the differences in slopes and the1/f alpha coefficients for phase shifting vs. phase synchrony as well as the average $\alpha \approx 1$.

Table II shows the alpha slope values and age regression correlations and t-tests between the spectral distributions for phase shift vs. phase synchrony intervals for the four sample subjects in figure 6. The α values for phase shift were statistically significantly smaller than the α values for phase synchrony and the average α value was close to 1.0 which indicates that decomposition of the log-log spectral distribution into sub-components of phase shift vs. phase synchrony is useful in order to reveal more of the underlying EEG dynamics.

Table II

Linear Regressions of Log-Log Spectral Analyses of Phase Shift and Phase Synchrony

REGRESSIONs	Subject 1	Subject 2	Subject 3	Subject 4
Locking - α	1.4223	1.3207	1.3764	1.2088
Shift - α	0.8226	0.7453	0.6826	0.7938
Average - α	1.1225	1.0330	1.0295	1.0013
T-Test	p < .0001	p < .0001	p < .0001	p < .0001

Table II- Summary of the log-log regression fits and estimates of the slope (i.e., alpha) for the same subjects as in figs. 5 & 6. The alpha values in the $1/f^{\alpha}$ distributions are shown for the phase synchrony vs. phase shift periods. The average α values were near to 1.0. The sub-component analyses of phase shift vs. phase synchrony reveals interesting differences in the slope or alpha of the 1/f distribution for phase shift vs. phase synchrony.

3.2 – Development of Phase Shift Duration

Figure 7 shows the mean duration of phase shift in the alpha frequency band from 0.44 to 16.22 years of age. The top row are mean phase shift duration values in the anterior-to-posterior direction (see fig. 1) and the bottom row are the posterior-to-anterior electrode combinations. The left column are the mean phase reset durations for the left hemisphere and

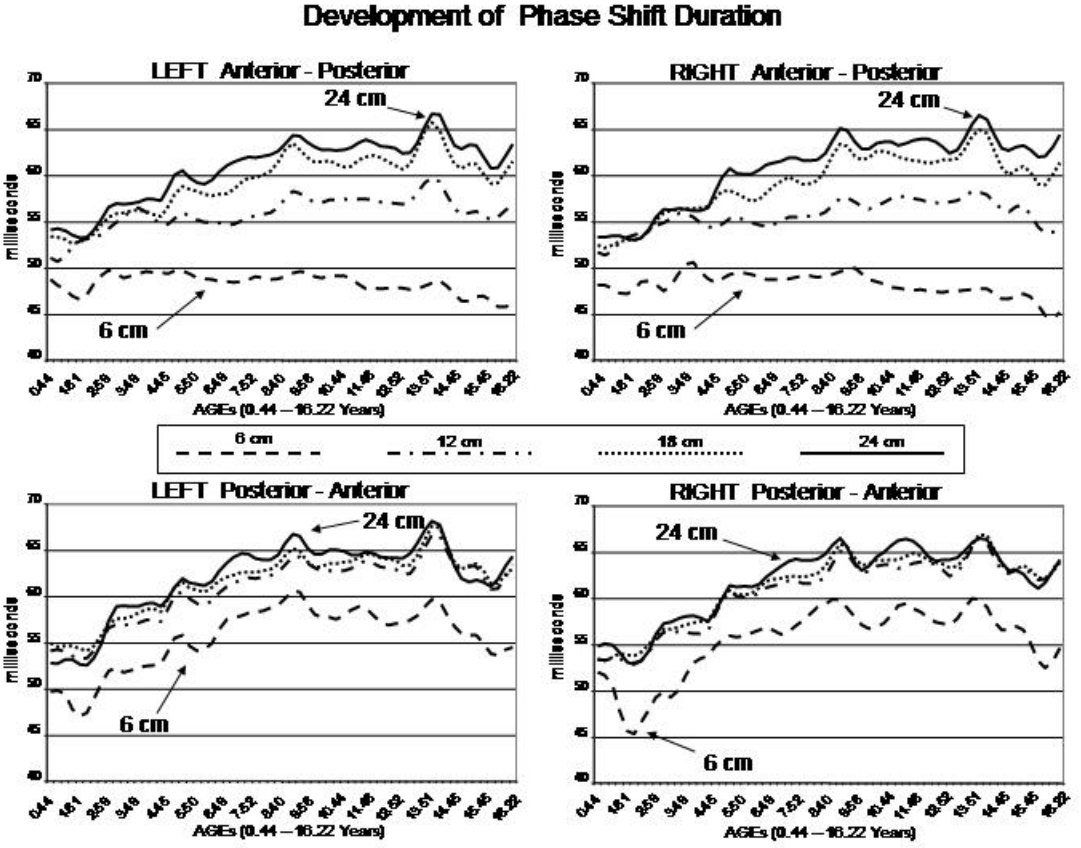

Fig. 7- Mean EEG phase shift duration from 0.44 years of age to 16.22 years of age. Top row are from the anterior-to-posterior electrode combinations and bottom row are from the posterior-to-anterior electrode combinations (see Fig. 1). The left column is from the left hemisphere and the right column is from the right hemisphere. It can be seen that phase shift duration increases in most electrode combinations but decreases in the short inter-electrode distance (6 cm) in the anterior-to-posterior direction.

the right column are the right hemisphere values. It can be seen that there were oscillations and sudden changes in the mean duration of phase shift and there was a steady increase in the mean duration of phase shift as a function of age in the long inter-electrode distances (18 cm & 24 cm) and reduced phase shift duration in the short inter-electrode distance (6 cm) in anterior-posterior directions. In the posterior-anterior direction, an increase in phase shift duration was present as a function of age in all inter-electrode distances, although the long inter-electrode distances (18 cm & 24 cm) exhibited a more pronounced increase in phase duration with age than the short inter-electrode distances (6 cm).

Table III shows the results of a linear fit of the mean duration of phase shift as a function of age for all electrode pairings. It can be seen in Table III that there were statistically significant negative slopes in the short inter-electrode distance (6 cm) in the anterior-posterior direction and positive slopes

in all other instances. Statistically significant age regressions were present for all of the developmental trajectories.

Table III

Age Regression of Phase Shift Duration

LEFT Anterior - Posterior

	6cm	12cm	18cm	24cm
SLOPE	-0.0001	0.0003	0.0005	0.0005
INTERCEPT	0.0494	0.0536	0.0544	0.0554
CORRELATION	-0.534	0.700	0.833	0.914
SIGNIFICANT	P<.0001	P<.0001	P<.0001	P<.0001

RIGHT Anterior - Posterior

	6cm	12cm	18cm	24cm
SLOPE	-0.0002	0.0002	0.0005	0.0007
INTERCEPT	0.0494	0.0538	0.0543	0.0548
CORRELATION	-0.577	0.633	0.823	0.861
SIGNIFICANT	P<.0001	P<.0001	P<.0001	P<.0001

LEFT Posterior - Anterior

	6cm	12cm	18cm	24cm
SLOPE	0.0005	0.0005	0.0005	0.0005
INTERCEPT	0.0516	0.0565	0.0564	0.0554
CORRELATION	0.634	0.731	0.819	0.914
SIGNIFICANT	P<.0001	P<.0001	P<.0001	P<.0001

RIGHT Posterior - Anterior

	6cm	12cm	18cm	24cm
SLOPE	0.0005	0.0007	0.0007	0.0007
INTERCEPT	0.0511	0.0563	0.0555	0.0548
CORRELATION	0.628	0.771	0.841	0.861
SIGNIFICANT	P<.0001	P<.0001	P<.0001	P<.0001

Table III – Linear regression statistics for mean phase shift duration from 0.44 years to 16.22 years of age.

The top two rows are from the anterior-to-posterior direction and the bottom two rows are from the posterior-to-anterior direction. Short Inter-electrode distance (6 cm) in the anterior-to-posterior direction exhibited a negative slope as a function of age while all other inter-electrode distances and direction exhibited positive slopes as a function of age. The y-intercept, regression correlation and statistical significance are also shown.

Multivariate analyses of variance (MANOVA) were conducted with the factors being direction (anterior-to-posterior vs. posterior-to-anterior), left hemisphere vs. right hemisphere and distance (6 cm, 12 cm, 18 cm & 24 cm). No significant left vs. right hemisphere affect was present ($F= 0.2345$, $P < 0.628$). However, there was a statistically significant direction affect ($F = 303.73$, $P < .0001$) with a statistically significant Bonferroni post hoc test ($P < .0001$). There was also a statically significant distance affect ($F = 350.21$, $P < .0001$) with statistically significant Bonferroni post hoc tests ($P > ,0001$) for all inter-electrode distances except for 24 cm – 18 cm ($P < 0.68$).

3.3 – Development of the Phase Synchrony Interval

Figure 8 shows the mean phase synchrony interval in the alpha frequency band from 0.44 to 16.22 years of age. The top row are mean phase synchrony interval values in the anterior-to-posterior direction (see fig. 1) and the bottom row are the posterior-to-anterior electrode combinations. The left column are the mean phase synchrony intervals for the left hemisphere and

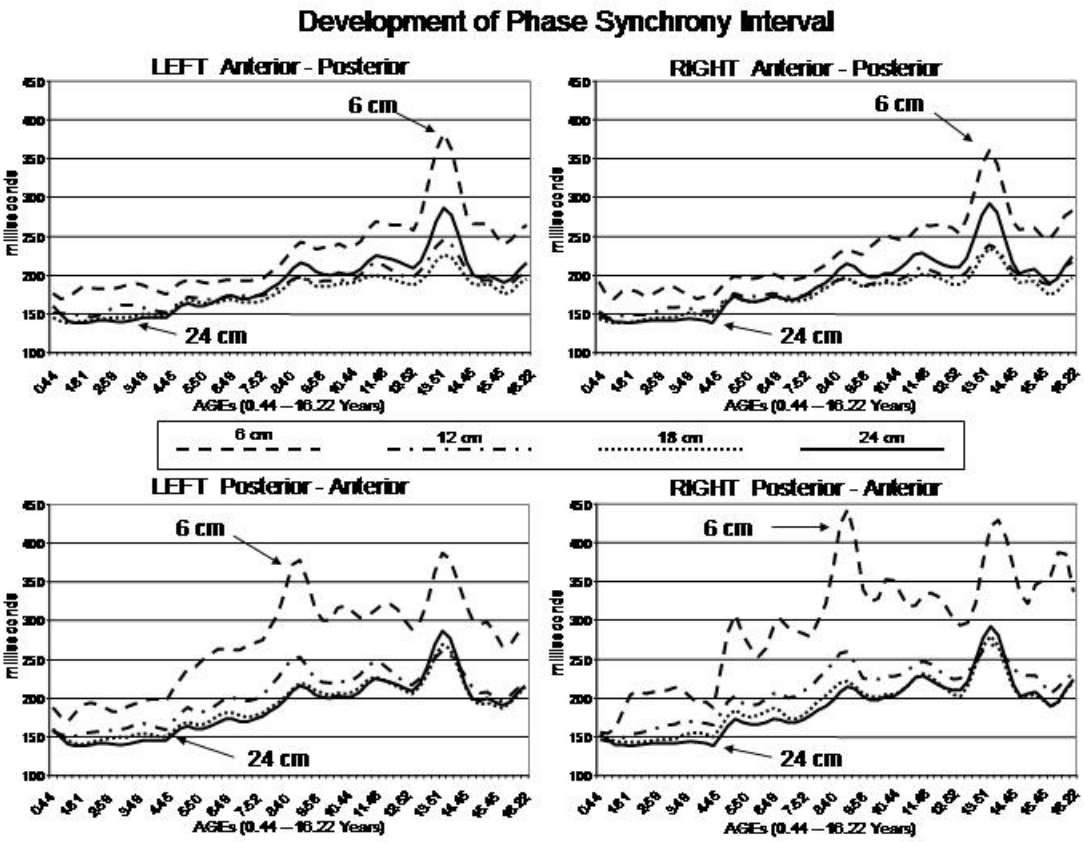

Fig. 8- Mean EEG phase synchrony intervals from 0.44 years of age to 16.22 years of age. Top row are from the anterior-to-posterior electrode combinations and bottom row are from the posterior-to-anterior electrode combinations (see Fig. 1). The left column is from the left hemisphere and the right column is from the right hemisphere. Growth spurts and oscillations during development are seen. Also, it can be seen that phase synchrony intervals increase as a function of age in all electrode combinations.

the right column are the right hemisphere values. It can be seen that there were oscillations and sudden changes in the mean phase synchrony intervals and there was a steady increase in the mean phase synchrony interval as a function of age in the short inter-electrode distance (6 cm) with less increased phase synchrony intervals in the long inter-electrode distances. Sudden increases in the mean phase synchrony interval were present n all electrode combinations at ages 9 and 14 years, especially in the short inter-electrode distances (6 cm) and in the posterior-to-anterior direction.

Table IV shows the results of a linear fit of the mean phase synchrony interval as a function of age for all electrode pairings. It can be seen in Table IV that there were statistically significant positive slopes in all instances. The short inter-electrode distance (6 cm) exhibited a steeper developmental slope in the posterior-to-anterior direction than in the anterior-to-posterior direction.

Table IV

Age Regression of Phase Synchrony Interval

LEFT Anterior - Posterior

	6cm	12cm	18cm	24cm
SLOPE	0.0057	0.0045	0.0043	0.0065
INTERCEPT	0.1559	0.1457	0.1352	0.1324
CORRELATION	0.825	0.852	0.868	0.831
SIGNIFICANT	P<.0001	P<.0001	P<.0001	P<.0001

RIGHT Anterior - Posterior

	6cm	12cm	18cm	24cm
SLOPE	0.0057	0.0047	0.0044	0.0063
INTERCEPT	0.1538	0.1448	0.1355	0.1308
CORRELATION	0.870	0.885	0.859	0.840
SIGNIFICANT	P<.0001	P<.0001	P<.0001	P<.0001

LEFT Posterior - Anterior

	6cm	12cm	18cm	24cm
SLOPE	0.0101	0.0055	0.0056	0.0065
INTERCEPT	0.1871	0.1568	0.1419	0.1324
CORRELATION	0.783	0.781	0.815	0.831
SIGNIFICANT	P<.0001	P<.0001	P<.0001	P<.0001

RIGHT Posterior - Anterior

	6cm	12cm	18cm	24cm
SLOPE	0.0131	0.0063	0.0059	0.0063
INTERCEPT	0.1867	0.1566	0.1423	0.1308
CORRELATION	0.824	0.833	0.821	0.840
SIGNIFICANT	P<.0001	P<.0001	P<.0001	P<.0001

Table IV – Linear regression statistics for mean phase synchrony intervals from 0.44 years to 16.22 years of a The top two rows are from the anterior-to-posterior direction and the bottom two rows are from the Posterior-to-anterior direction. The y-intercept, regression correlation and statistical significance are also shown.

Multivariate analyses of variance (MANOVA) were conducted with the factors being direction (anterior-to-posterior vs. posterior-to-anterior), left hemisphere vs. right hemisphere and distance (6 cm, 12 cm, 18 cm & 24 cm). No significant left vs. right hemisphere affect was present ($F= 3.033$, $P < 0.082$). However, there was a statistically significant direction affect ($F = 82.02$, $P < .0001$) with a statistically significant Bonferroni post hoc test ($P < .0001$). There was also a statically significant distance affect ($F = 173.55$, $P < .0001$) with statistically significant Bonferroni post hoc tests ($P >$,0001) for all inter-electrode distances except for 24 cm – 12 cm ($P < 0.271$) and 24 cm – 18 cm ($P < 0.783$).

3.4- Relations Between EEG Phase Reset and Coherence

Coherence is a measure of phase stability and one would expect a positive correlation between the duration of phase synchrony and coherence. We tested this hypothesis using a Pearson product correlation coefficient of the developmental time series of coherence and phase shift duration and phase synchrony interval in the short inter-electrode distances (6 cm). Table V shows the average correlation of the short inter-electrode distance measures in which there was a negative correlation between coherence and phase shift duration (i.e., inverse relationship to "Chaos) and a positive correlation between coherence and phase synchrony intervals (i.e., direct relationship to "Stability"). As expected there was an inverse relationship between phase shift duration ("chaos") and phase synchrony interval ("stability") however, the correlations were relatively small indicating that the majority of variance is unaccounted for when correlating phase shift duration with phase synchrony interval. Importantly, the hypothesis of a positive relationship between coherence and phase synchrony was confirmed. As seen in Table V, correlation analyses of the long inter-electrode distance (24 cm) were positive for both phase shift duration and phase synchrony interval.

Table V

Correlations Between Coherence and Phase Shift (Chaos) and Phase Synchrony (Stability)

	Chaos	Stability
Coherence	- 0.547	0.863
Chaos	———	- 0.386
Stability	- 0.386	———

Table V- Average correlations between coherence and phase shift duration ("Chaos") and phase synchrony ("Stability") at the short inter-electrode distance (6 cm). There was a negative correlation between coherence and "chaos" and a positive correlation between coherence and "stability".

3.5 – Developmental Oscillations

Examination of figures 7 and 8 shows ultra-slow oscillations with inter-peak intervals of approximately 2 to 3 years. Spectral analyses of the developmental time series of mean duration of phase shift from 0.44 years to 16.22 years for the 6 cm and 24 cm inter-electrode distances are shown in figure 9. The top row are the frontal-to-posterior electrode combinations and the bottom row are the occipital-to-anterior combinations. The left column are the left hemisphere mean FFT values and the right column are the right hemisphere values (see Fig. 1). In general there was greater developmental spectral energy in the short inter-electrode distance (6 cm) in comparison to the long inter-electrode distance (24 cm). Most of the developmental spectral energy was in the ultraslow frequency range of 1 cycle per lifespan (i.e., a wavelength of 16 years) to approximately 12 cycles per lifespan (i.e., a wavelength of 1.33 years). The highest peak frequency was 31 cycles per lifespan (i.e., a wavelength of 0.51 years or 6.12 months).

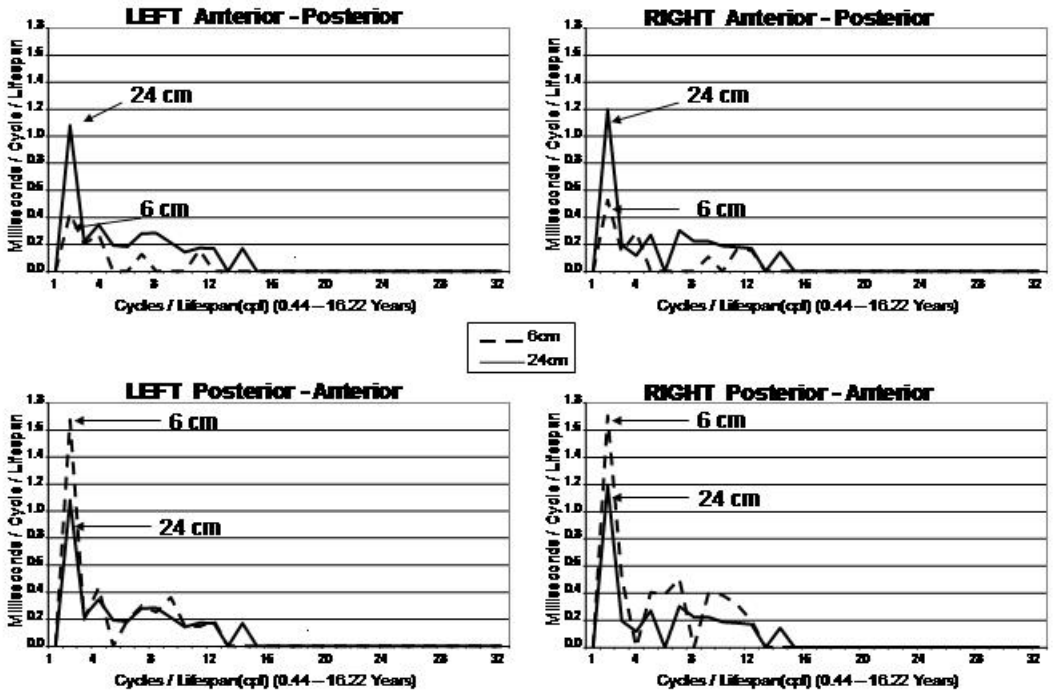

Fig. 9 – Fourier spectral analyses of the developmental trajectories of phase shift duration from 0.44 years to 16.22 years of age in short (6 cm) (solid line) and long (24 cm) (dashed line) inter-electrode distances in the anterior-to-posterior and posterior-to-anterior directions. Magnitude is on the y-axis and frequency on the x-axis. Distant inter-electrodes exhibited greater power in the anterior-to-posterior direction while local connections exhibited the greater power in the posterior-to-anterior direction.

Spectral analyses of the developmental time series of mean phase synchrony intervals from 0.44 years to 16.22 years for the 6 cm and 24 cm inter-electrode distances are shown in figure 10. The top row of figure 10 are the anterior-to-posterior electrode combinations and the bottom row are the posterior-to-anterior combinations. The left column are the left hemisphere FFT values and the right column are the right hemisphere values (see Fig. 1). Similar to phase shift duration, phase synchrony exhibited most of the spectral energy in the ultraslow frequency range of 1 cycle per lifespan (i.e., a wavelength of 16 years) to approximately 20 cycles per lifespan (i.e., a wavelength of 0.8 years). Similar to phase shift duration, phase synchrony in the short inter-electrode distance (6 cm) was greater than the long distance (24 cm) in the posterior-to-anterior direction.

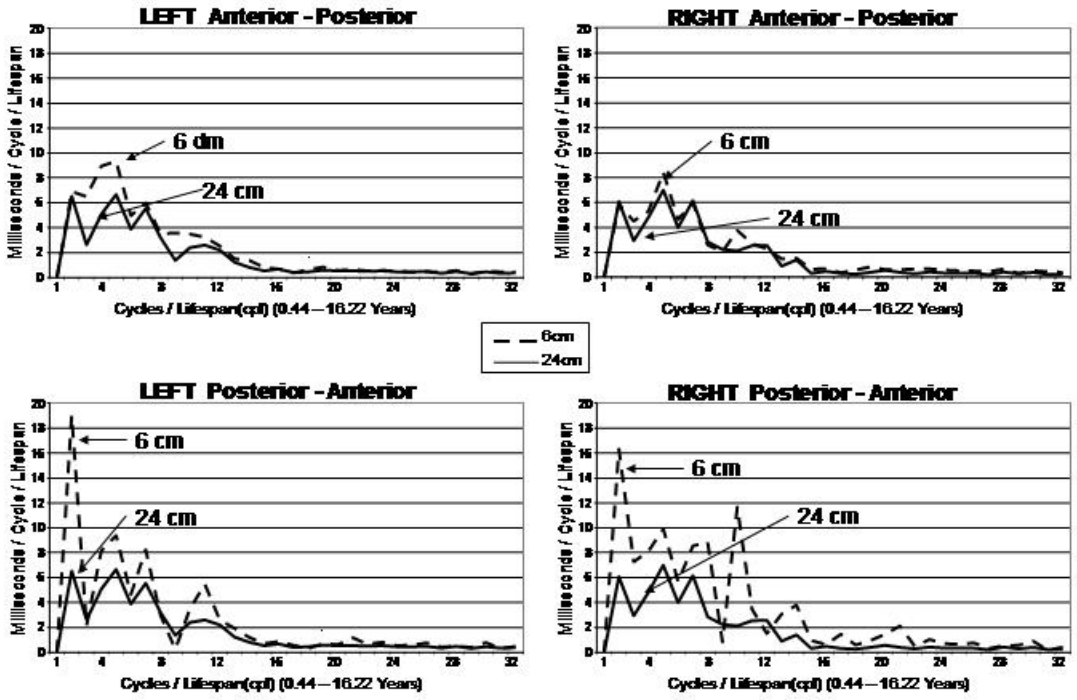

Fig. 10 – Fourier spectral analyses of the developmental trajectories of mean phase synchrony from 0.44 years to 16.22 years of age in short (6 cm) (solid line) and long (24 cm) (dashed line) inter-electrode distances in the anterior-to-posterior and posterior-to-anterior directions. Magnitude is on the y-axis and frequency on the x-axis. The greatest spectral energy was in the short distance inter-electrodes (6 cm) in the posterior-to-anterior direction.

Tables VI and VII are summaries of the cycles per lifespan (cpl) and the wavelength (16 yrs/cpl) of the spectral peaks in the FFT analyses of the mean duration of phase shift and mean phase synchrony developmental trajectories from 0.44 years to 16.22 years. Table VI shows the FFT peak values in the frontal-to-posterior direction for both coherence (Top) and phase differences (Bottom) and Table VII shows the values in the posterior-to-anterior direction. It can be seen that short (6 cm) and distant (24 cm) are different for coherence vs. phase in both directions. In general there are more spectral peaks and greater power in the short distant inter-electrode connections in coherence than there are in phase differences at 6 cm. The opposite is true for the development of phase differences which exhibited more spectral peaks and greater power in the long distance inter-electrode connections than are in coherence at 24 cm.

Table VI
Summary of Spectral Peaks of Phase Shift Duration

Anterior - Posterior

LEFT			
	6cm		24cm
CPL	λ (yrs)	CPL	λ (yrs)
2	8	2	8
4	4	4	4
7	2.29	7	2.29
11	1.45	8	2
		12	1.33
		14	1.14

RIGHT			
	6cm		24cm
CPL	λ	CPL	λ (yrs)
2	8	2	8
4	4	5	3.2
9	1.78	7	2.29
11	1.45	12	1.33
		14	1.14

Posterior - Anterior

LEFT			
	6cm		24cm
CPL	λ (yrs)	CPL	λ (yrs)
2	8	2	8
4	4	4	4
7	2.29	7	2.29
9	1.78	14	1.14
12	1.33		

RIGHT			
	6cm		24cm
CPL	λ (yrs)	CPL	λ (yrs)
2	8	2	8
5	3.2	5	3.2
7	2.29	7	2.29
9	1.78	14	1.14
10	1.6		

Table VI– Summary of spectral peaks of the phase shift duration in the anterior-to-posterior direction (top) and the posterior-to-anterior direction (bottom) for 6 cm and 24 cm inter-electrode distances. , lifespan = 16 years and cpl = cycles per lifespan and λ = wavelength in years or lifespan/cpl.

Table VII are summaries of the cycles per lifespan (cpl) and the wavelength (16 yrs/cpl) of the spectral peaks in the FFT analyses of the mean phase synchrony developmental trajectories from 0.44 years to 16.22 years. There largest number of spectral peaks was in the posterior-to-anterior direction in the short inter-electrode distance (6 cm).

Table VII

Summary of Spectral Peaks of Phase Synchrony Interval

Anterior - Posterior

LEFT			
	6cm		24cm
CPL	λ (yrs)	CPL	λ (yrs)
2	8	2	8
4	4	5	3.2
5	3.2	7	2.29
7	2.29	11	1.45

RIGHT			
	6cm		24cm
CPL	λ (yrs)	CPL	λ (yrs)
2	8	2	8
5	3.2	5	3.2
7	2.29	7	2.29
10	1.6	12	1.33

Posterior - Anterior

LEFT			
	6cm		24cm
CPL	λ (yrs)	CPL	λ (yrs)
2	8	2	8
5	3.2	5	3.2
7	2.29	7	2.29
11	1.45		
21	0.76		

RIGHT			
	6cm		24cm
CPL	λ (yrs)	CPL	λ (yrs)
2	8	2	8
5	3.2	5	3.2
8	2	7	2.29
10	1.6	12	1.33
14	1.14	14	1.14
21	0.76		

Table VII – Summary of spectral peaks of phase synchrony intervals in the anterior-to-posterior direction (top) and the posterior-to-anterior direction (bottom) for 6 cm and 24 cm inter-electrode distances. Lifespan = 16 years and cpl = cycles per lifespan, and λ = wavelength in years or lifespan/cpl.

4.0 – Discussion

4.1 – Self-Organized Criticality and Phase Reset

The process of EEG phase reset was spontaneous, repetitive and pervasive in all subjects in this study and is thus a general property of the human EEG. Although pervasive and spontaneous, nonetheless, an important finding is that the average phase shift duration and the average phase synchrony interval significantly correlated with age and exhibited different maturational trajectories in the anterior-to-posterior vs. posterior-to-anterior scalp locations (see fig. 1). The results of this study are consistent with Self-Organized Criticality (SOC) models of cortical function (Bak et al, 1988; Freeman et al, 2003; 2006; Linkenkaer-Hansen et al, 2001; Le van Quyen, 2003; Stam and de Bruin, 2004; Buzsaki, 2006). Self-Organized Criticality was defined by Bak et al (1988) as the combination of "self-organization" and "criticality" necessary to describe complicated systems in which phase transitions spontaneously occur without external "tuning" or influences. A fundamental property of

SOC is the presence of $1/f^{\alpha}$ distributions that characterize invariant scaling properties, fractal spatial statistics and long-range temporal correlations, where f = frequency and $\alpha \approx 1$ (Bak et al, 1988; Nikulin and Brismar, 2004, 2005; Parish et al, 2004). According to studies by Rios and Zhang (1999) the "pink noise" $1/f^{\alpha}$ distribution is the result of a mixture of a slow process of energy addition and a fast process corresponding to the redistribution of energy. Rios and Zhang (1999) also showed that $1/f^{\alpha}$ and SOC require a preferred propagation direction and a limited range of energy dissipation. EEG phase reset meets the slow and fast component criteria with rapid phase shift onsets as a "fast process" (5 msec – 20 msec) and phase synchrony as a comparative "slow process" (150 msec to 1 second; Freeman et al, 2006). Feigenbaum (1983) evaluated nonlinear systems in "criticality transitions" during the period of transition from quasi-periodic behavior to "chaos" and discovered that the expansion around this point is a $1/f^{\alpha}$ distribution. In other words the complex state at the border between predictable oscillatory behavior and completely unpredictable chaos is the "Pink Noise" distributions called "one-over-f " or 1/f . As pointed out by Bak et al (1988); Freeman et al (2003; 2006) and Buzsaki (2006) the brain approaches "chaos" followed by a transition to periods of synchrony. Understanding the details of the Feigenbaum's "Critical Point" during the step toward transition from predictable behavior to "Chaos" is referred to as the Universality principle that was expanded by Haken (1983) to a general mathematical solution using a small set of "order parameters" to control the behavior of higher ordered systems. Once the value of the exponent in the $1/f^{\alpha}$ equation is known then the mathematics of SOC are more tractable (Rios and Zhang, 1999; Pikovsky et al, 2003).

4.2 – Long-Range Temporal and Spatial Correlations

As emphasized by Buzaki (2006) and Freeman et al (2003; 2006) an attractive feature of SOC is its ability to describe complicated systems behavior by simple power laws. The presence of the $1/f^{\alpha}$ distribution is a tell tale sign of self-organization and also measures the length of the correlation or "temporal memory effects" in the EEG signal. The slope of the log-log fit to the spectral distribution is an estimate of the temporal-range of the correlation in which the closer the slope approximates 1.0 then the stronger the long-range spatial and temporal correlations (Nikulin and Brismar, 2005; Stam and de Bruin, 2004). In the present study we showed that the two components of phase reset (i.e., phase shift and phase synchrony) exhibit different α coefficient values in the $1/f^{\alpha}$ function where phase synchrony spectra exhibited a shorter temporal memory effect while the phase shift spectra (i.e., "chaos") exhibited a longer-range temporal memory (see fig. 6 and Table II). The linear scale invariant properties of 1/f reflect the temporal dependence of events that pre-date the occurrence of critical events and in the case

of EEG phase synchrony there is reduced influence by past events. In contrast, the period of phase shift when the brain approaches "chaos" is a period of high uncertainty with a long-range temporal memory. The findings in this study show that there are orderly genetic laws that govern the postnatal development of SOC. The rhythmic order and linear shifts are likely supported by fundamental DNA-RNA molecular processes involved in synaptogenesis (Thatcher et al, 1987; 1992; 1994; 1998).

4.3 – Phase Reset in Local versus Distant Connection Systems

The short inter-electrode distance (6 cm) exhibited stronger developmental changes in the mean phase synchrony interval than the long inter-electrode distance (24 cm), especially in the posterior-to-anterior direction. The short inter-electrode distance (6 cm) also exhibited larger growth spurts in phase synchrony intervals than the long inter-electrode distance connections (24 cm) (see fig 8). In contrast to phase synchrony, the mean phase shift duration declined in the local frontal connections while it increased in the long inter-electrode distance (24 cm) in the anterior-to-posterior direction (see fig. 7). This indicates that local frontal connections exhibit shorter periods of phase shift duration (i.e., less"chaos") and longer periods of phase synchrony as a function of age. In general, long distance connection systems exhibited longer phase shift durations (i.e., more "Chaos") than local connection systems. The finding that phase synchrony intervals only modestly increased with age in the long distance systems but strongly increased in the local connection systems indicates that maturation is dominated more by local phase synchrony than are the long distance systems. The relations between local and distant populations of neurons is critical in understanding how the neocortex spatially and temporally scales functions that are localized and connected by long distant fiber systems.

Previous studies have used two compartmental models of EEG coherence in which the number of connections and the strength of connections influence the magnitude of coherence (Nunez, 1981; Thatcher et al, 1986; 1998; 2007; McAlaster, 1992; Hanlon and Thatcher, 1999Van Beijsterveldt et al 1998; van Baal et al, 2001). A positive correlation between coherence and phase synchrony is expected since coherence is a measure of phase synchrony (Otnes and Enochson, 1978; Bendat and Piersol, 1980). Also, one would expect a negative correlation between phase shift duration and coherence since phase shift duration is related to unpredictability and a lack of phase synchrony (i.e, "Chaos"). This study showed a significant positive correlation between phase synchrony intervals ("stability") and coherence and a negative correlation to phase shift duration ("chaos"), especially in the local or short inter-electrode pairs. It would be consistent with EEG coherence studies (Thatcher et al, 1986; 1998; 2007; McAlaster, 1992; van Ball et al, 2001; Van Beijsterveldt et al, 1998) to argue that as the number

of connections increases with age then there is increased coherence and increased stability and decreased "chaos". The findings in the present study are consistent with this hypothesis. A simple mathematical model that links the development of the number and/or density of synaptic connections to EEG coherence (Thatcher, 1994; Thatcher et al, 2007) and to the two components of phase reset, i.e., "Chaos" and "Stability" is shown in equation 1:

Eq. 1 $$N_{ij} \Rightarrow K \frac{S_{ij}}{C_{ij}}$$

Where N_{ij} = the number and/or density of local synaptic connections in a matrix, K = a proportionality constant, S_{ij} = the "Stability" or phase synchrony and C_{ij} = "Chaos" or phase shift duration. Although this is a two-way relationship during short periods of time, the arrow symbol $\Rightarrow$ represents the developmental trend which gives greater weight to the relationship between the number of synaptic connections as influencing "chaos" and "stability" rather than the reverse direction. Certainly, neural synchrony is important for learning and perception and memory and thus the environment must be an important factor in determining the number of connections between different brain regions. However, there were oscillations and growth spurts in phase reset over the lifespan from environmentally diverse subjects and thus, there is greater overall weight given to the number and/or density of synaptic connections as determining the balance between "chaos" and "stability" over the maturation period from infancy to adolescence. That is, as the number of synaptic connections increases then phase stability increases and the duration of phase reset decreases. It is known that there are a specific set of molecular mechanisms that produce and eliminate synaptic connections and these same mechanisms operate from mollusks to humans (Kandel, 2007). The general pathway of DNA-RNA and protein synthesis to produce synaptic connections between neurons is essentially phylogenetically universal and under control of epigenetic processes that unfold in an orderly process during human maturation. Nonlinear ecological models of cooperation, competition, independence and predator/prey have been applied to measures of human cortical development with highly significant statistical fits (Thatcher, 1994; 1998). The findings in this study generally support SOC epigenetic models of human brain development where growth spurts are punctuations or "chaos" within periods of stability and the underlying 1/f dynamics represent long-range temporal and spatial correlations. The linkage of the number and/or density of synaptic connections to SOC suggests that the number of synaptic connections

may be one of the critical order parameters that determines the dynamics of the cortico-cortical coupling during human development.

4.4 – Differences in the anterior-to-posterior versus the posterior-to-anterior direction

The most striking difference between the anterior-to-posterior vs. the posterior-to-anterior direction of electrode placement are the phase shift duration and phase synchrony interval differences in the short inter-electrode distances (6 cm). The development of EEG phase shift duration in the anterior-to-posterior direction exhibited a negative slope with age, whereas the 6 cm short distance electrode combination exhibited a positive slope with age in the posterior-to-anterior direction. The development of phase synchrony intervals were also different in the short inter-electrode distance (6 cm) in the anterior-to-posterior vs. the posterior-to-anterior directions. Local or short inter-electrode distances exhibited larger growth spurts (age 9 and age 14) in the posterior-to-anterior direction than in the anterior-to-posterior direction. These findings are consistent with a differential preference for packing density in local brain regions. For example, the occipital brain regions have the highest neural packing density and the frontal lobes have the lowest packing density (Blinkov and Glezer, 1968; Carpender and Sutin, 1983). The number of connections is related to the packing density by virtue of the available area on dendrites for synaptogenesis (Purves, 1988). Although high packing density can result in shorter dendrites, nonetheless, with more neurons there are more synaptic connections and thus the anterior-to-posterior greater phase duration is due to a lower number of synaptic connections in the frontal lobes in comparison to the occipital lobes. These findings are consistent with equation 1, where reduced connections are related to increased periods of "chaos" and increased number of connections is related to longer synchronization intervals and shorter periods of "chaos".

4.5 – Nonlinear Oscillations in SOC and Growth Spurts

The frequency spectrum of the development of phase shift duration and phase synchrony intervals (SOC) showed significant ultraslow oscillations over the lifespan from infancy to adolescence. The mean frequency of oscillations were different in the anterior-to-posterior and posterior-to-anterior directions but very similar for different inter-electrode distances and for left and right hemispheres. The strongest spectral magnitudes for the development of phase shift duration and phase synchrony were repetitive cycles at wavelengths between 8 years and 2 years. The highest frequency of oscillations were approximately 1 year wavelengths and the higher frequency oscillations exhibited the lowest power.

The presence of relatively rapid changes in phase shift duration and phase synchrony intervals at specific postnatal ages, e.g., 9 years and 14 years (see figs. 7 & 8) is evidence of nonlinear growth spurts that are hypothesized to involve rapid changes in the number and/or density of synaptic connections (see equation 1). Likely competitive, cooperative and predator/prey dynamics are ecological factors that underlie the rapid changes in phase reset as well as coherence and phase (Thatcher, 1994; 1998; Thatcher et al, 2007). The nonlinear Lotka-Volterra predator/prey equations (Thompson and Stewart, 1986; Berryman, 1981; Thatcher, 1998) are often used to model competitive and cooperative network dynamics and are likely useful equations for the study of the development of SOC and EEG coherence and phase.

An important fact is that there was a diversity of different environments and experiences in the lives of all of the 458 subjects in this study. In other words, the regularity of growth spurts and the strength of the repetitive cycles of phase shift duration and phase synchrony can not be explained by a single environmental factor. The most likely explanation is that a common genetic factor is responsible for the regular rhythms and slopes of change in phase reset over a 16 year period of time. The findings in this study are consistent with earlier studies from this laboratory demonstrating ultraslow oscillations and growth spurts in EEG coherence and phase differences (Thatcher et al, 1987; Thatcher, 1992; 1994; 1998; 2007; Hanlon et al, 1999; McAlaster, 1992) as well as genetic studies of the relative rates of development of local vs. distance coherence measures (Van Beijsterveldt et al, 1998; van Baal et al, 2001). The studies by Van Beijsterveldt et al (1998) and van Baal et al (2001) demonstrated different genetic contributions to local vs. distant connections in which there is more genetic influence on distant connections than on local connections but both compartments dynamically evolve with growth spurts at specific ages. To the best of our knowledge no genetic studies of phase shift duration or phase synchrony intervals have been conducted. If such studies show a significant genetic component governing the development of phase reset then models of driving force oscillator systems can be considered with the DNA and RNA molecules principally responsible for the production and pruning of the number of connections over a lifespan. As mentioned previously, correlation and factor analyses of coherence and phase reset reveal statistically significant relationships in which increased coherence in local brain regions is inversely related to phase shift duration and positively related to phase shift synchrony. These findings suggest a relationship between oscillations in the number of connections and the length of phase stability over a 16 year period likely governed by systems of coupled nonlinear dynamical oscillators.

5.0 – References

Bak, P., Tang, C. and Wisenfeld, K. (1988). Self-organized criticality. Physical Rev. A. 38(1): 364-374.

Bak, P. (1996). How Nature Works: The science of Self-Organized Criticality. Springer-Verlag, New York.

Berryman, A. A. (1981). *Population systems: A general introduction.* New York: Plenum Press.

Beggs, J.M. and Plenz, D. (2003). Neuronal avalanches in neocortical circuits. J. Neurosci., 23: 11167-11177.

Bendat, J. S. & Piersol, A. G. (1980). *Engineering applications of correlation and* spectral analysis. New York: John Wiley & Sons.

Blinkov, S. M. and Glezer, I., (1968). The Human Brain in Figures and Tables: A Quantitative Handbook, Basic Books, Inc., Publisher Plenum Press.

Bloomfield, P. (2000). Fourier Analysis of Time Series: An Introduction, John Wiley & Sons, New York.

Breakspear, M. and Terry, J.R. (2002a). Detection and description of non-linear interdependence in normal multichannel human EEG data. Clin. Neurophysiol., 113(5): 735-753.

Breakspear, M. and Terry, J.R. (2002b). Nonlinear interdependence in neural systems: motivation, theory and relevance. Int. J. Neurosci., 112(10): 1263-1284.

Breakspear, M. (2002). Nonlinear phase desynchronization in human electroencephalographic data. Hum. Brain Mapp., 15(3): 175-198.

Breakspear, M. (2004). Dynamic connectivity in neural systems: theoretical and empirical considerations. Neuroinformatics, 2(2): 205-226.

Buzsaki, G. and Draguhn, A. (2004). Neuronal oscillations in cortical networks. Science, 304(5679): 1926-1929.

Buzsaki, G. (2006). Rhythms of the Brain, Oxford Univ. Press, New York.

Bruns, A. (2004). Fourier, Hilbert and wavelet-based signal analysis: are they really different approaches? J. Neurosci. Methods, 137(2): 321-332.

Carpenter, M.B. and Sutin, J. (1983). Human Neuroanatomy, 8th edition, Williams and Wilkins, Baltimore, Maryland.

Chavez, M., Le Van Quyen, M., Navarro, V., Baulac, M. and Martinerie, J. (2003). Spatio-temporal dynamics prior to neocortical seizures: amplitude versus phase couplings. IEEE Trans. Biomed. Eng. 50(5): 571-583.

Chialvo, D.R. and Bak, P. (1999). Learning from mistakes. Neuroscience, 90:1137-1148.

Cooper R, Winter AL, Crow HJ and Walter WG. (1965). Comparison of subcortical, cortical and scalp activity using chronically indwelling electrodes in man. Electroencpehalogr Clin Neurophysiol. 18:217-222.

Cosmelli, D., David, O., Lachaux, J.P., Martinerie, J., Garnero, L., Renault, B. and Varela, F. (2004). Waves of consciousness: ongoing cortical patterns during binocular rivalry. Neuroimage, 23(1): 128-140.

Damasio, A.R. (1989). Time-locked multiregional retroactivation: A systems-level proposal for the neural substrates of recall and recognition. Cognition, 33: 25-62.

Feigenbaum, M.J. (1983). Universal behavior in nonlinear systems. Physica, 7D: 16-19.

Freeman, W.J. (2003). Evidence from human scalp electroencephalograms of global chaotic itinerancy. Chaos, 13(3): 1067- 1077.

Freeman, W.J. and Baird, B. (1987). Relation of olfactory EEG to behavior: Spatial analysis. Behav. Neurosci., 101: 393-408.

Freeman w.J. and Rogers, L.J. (2002). Fine temporal resolution of analytic phase reveals episodic synchronization by state transitions in gamma EEGs. J. Neurophysiol, 87(2): 937-945.

Freeman, W.J., Burke, B.C. and Homes, M.D. (2003). Aperiodic phase re-setting in scalp EEG of beta-gamma oscillations by state transitions at alpha-theta rates. Hum Brain Mapp. 19(4):248-272.

Freeman, W.J., Homes, M.D., West, G.A. and Vanhatlo, S. (2006). Fine spatiotemporal structure of phase in human intracranial EEG. Clin Neurophysiol. 117(6):1228-1243.

Granger, C.W.J. and Hatanka, M. (1964). Spectral Analysis of Economic Time Series, Princeton University Press, New Jersey.

Hanlon, H. W., Thatcher, R. W. & Cline, M. J. (1999). Gender differences in the development of EEG coherence in normal children. *Developmental* Neuropsychology, *16* (3), 479-506.

Haken, H. 1983. “Synergetics, An Introduction”, Springer-Verlag, Berlin.

Jensen, O., and Lisman, J.E. (1998). An oscillatory short-term memory buffer model can account for data on the Sternberg task. J Neurosci. 18(24):10688-10699.

John, E.R. (2005). From synchronous neural discharges to subjective awareness? Progress in Brain Research, Vol. 150: 143-171.

Kahana, M.J. (2006). The cogntivie correlates of human brain oscillations. J. Neurosci., 26:1669-1672.

Kandel, E. R. (2007). In Search of Memory: The Emergence of a New Science of Mind. John Wiley & Sons, New York.

Kirschfeld, K. (2005). The physical basis of alpha waves in the electroencephalogram and the origin of the "Berger effect"., Biol. Cybem., 92(3):177-185.

Lachaux, J.-P., Rodriguez, E., Martinerie, J. anjd Varela, F.J. (1999). Measuring phase synchrony in brain signals. Hum. Brain Mapp. 8(4): 194-208.

Lachaux, J.-P., Rodriguez, E., Le Van Quyen, M., Lutz, A., Martinerie, J., Varela, F.J. (2000) Studying single-trials of phase synchronous activity in the brain. Int. J. Bifuc. Chaos, 10(10): 2429-2439.

Le Van Quyen, M., Foucher, J., Lachaux, J.-P., Rodriguez, E., Lutz, A., Martinerie, J. and Varela, F.J. (2001a). Comparison of Hilbert transform and wavelet methods for the analysis of neuronal synchrony. J. Neurosci. Methods, 111(2): 83-89.

Le Van Quyen, M., Martinerie, J., Navarro, V. and Varela, F.J. (2001b). Characterizing neurodynamic changes before seizures. J. Clin. Neurophysiol., 18(3): 191-208.

Le Van Quyen, M. (2003). Disentangling the dynamic core: A research program for a neurodynamics at the large-scale. Biol. Res., 36: 67-88.

Linkenkaer-Hansen, KI., Nikouline, V.V., Palva, J.M and Ilmoniemi, R.J. (2001). Long-range temporal correlations and scaling behavior in human brain oscillations. J. Neurosci. 21:1370-1377.

Lopes Da Silva, F.H. (1995). Dynamic of Electrical Activity of the Brain, Networks, and and Modulating Systems. In: P. Nunez, ed., *Neocortical Dynamics and Human EEG Rhythms*, 249-271.

Lopes Da Silva, F.H. and Pijn, J.P. (1995). Handbook of Brain Theory and Neural Networks. MIT Press, Arbib, Cambridge.

McAlaster, R. (1992). Postnatal cerebral maturation in Down's syndrome children: a developmental EEG coherence study, Int. J. Neurosci., 65(1-4): 221-2237.

McCartney, H., Johnson, A.D., Weil, Z.M. and Givens, B. (2004). Theta reset produces optimal conditions for long-term potentiation. Hippocampus, 14(6):684-697.

Netoff, T.I. and Schiff, S.J. (2002). Decreased neuronal synchronization during experimental seizures. J. Neurosci., 22(16): 7297-7307.

Niedermeyer, E. and Lopes da Silva, F. (1994). Electroencephalograph: Basic Principles, Clinical Applications and Related Fields, Wilkins and Williamson, Baltimore, Md.

Nikulin, V.V. and Brismar, T. (2004). Long-range temporal correlations in alpha nd beta oscillations: effect of arousal level and test-retest reliability. Clin. Neurophysiol., 115: 1896-1908.

Nikulin, V.V. and Brismar, T. (2005). Long-range temporal correlations in electroencephalographic oscillations: Relation to topography, frequency band, age and gender. Neurosci., 130: 549-558.

Nunez, P. (1981). Electrical Fields of the Brain. Oxford University Press, New York.

Nunez, P. (1994). Neocortical Dynamics and Human EEG Rhythms, Oxford University Press, New York.

Oppenheim, A.V. and Schafer, r.W. (1975). Digital Signal Processing, Printice-Hall, London.

Otnes, R.K. and Enochson, L. (1978). Applied Time Series Analysis, John Wiley & Sons, New York.

Parish, L.M., Worrell, G.A., Cranstun, S.D., Stead, S.M., Pennell, P. and Litt, B. (2004). Long-range temporal correlations in epileptogenic and non-epileptogenic human hippocampus. Neurosci., 125: 1068-1076.

Pikovsky, A., Rosenblum, M. and Kurths, J. (2003). Synchronization: A universal concept in nonlinear sciences. Cambridge Univ. Press, New York.

Purves, D. (1988). *Body and brain: A trophic theory of neural connections.* Boston: Harvard University Press.

Rios, L.P. and Zang, Y.C. (1999). Universal 1/f noise from dissipative self-organized criticality models. Phys. Rev. Let., 82(3): 472-475.

Rizzuto, D.S., Madsen, J.R., Bromfield, E.B., Schultz-Bonhage, A., Seelig, D., Aschenbrenner-Scheibe, R. and Kahana, M.J. (2003). Reset of human neocortical oscillations during a working memory task. Proc Natl Acad Sci U S A. 100(13):7931-7936.

Roelfsmema, P.R., Engel, A.K., Konig, P. and Singer, W. (1997). Visuomotor integraton is associated with zero time-lag synchronization among cortical areas. Nature, 385(6612): 157-161.

Rudrauf, D., Douiri, A., Kovach, C., Lachaux, J.P., Cosmelli, D., Chavez, A., Renault, B., Marttinerie, J. and Le Van Quyen, M. (2006). Frequency flows and the time-frequency dynamics of multivariate phase synchronization in brain signals. Neuroimage, 31: 209-227.

Savitzky, A. and Golay, M.J.E. (1964). Smoothing and differentiation of data by simplified least squares procedures, Analytic Chemistry, 36: 1627-1639..

Stam, C.J. and de Bruin, E.A. (2004). Scale-free dynamics of global functional connectivity in

the human brain. Hum. Brain Map. 22:97-109.

Stam, C.J. and de Bruin, E.A. (2004). Scale-free dynamics of global functional connectivity in the human brain. Hum. Brain Mapping, 22:97-109.

Tallon-Baudry, C., Bertrand, O., and Fischer, C. (2001). Oscillatory synchrony between human extrastriate areas during visual short-term memory maintenance. J. Neurosci., 21(20): RC177.

Tass, P.A. (1997). Phase Resetting in Medicine and Biology, Springer-Verlag, Berlin.

Tass, p.A., Rosenblum, M.G., Weule, J., Kurths, J., Pikovsky, A., Volkmann, J. aSchnitzler, A. and Freund, H.J. (1998). Detection of n:m phase locking from nosy data: application to magnetoencephalography. Phys. Rev. Lett., 81(15): 3291-3294.

Tesche, C.D. and Karhu, J. (2000). Theta oscillations index human hippocampal activation during a working memory task. Proc Natl Acad Sci U S A. 18;97(2):919-924.

Thatcher, R.W., Krause, P and Hrybyk, M. (1986). Corticocortical Association Fibers and EEG Coherence: A Two Compartmental Model. Electroencephalog. Clinical Neurophysiol., 64: 123 – 143.

Thatcher, R.W., Walker, R.A. and Guidice, S. (1987). Human cerebral hemispheres develop at different rates and ages. Science, 236: 1110-1113.

Thatcher, R.W. (1992). Cyclic cortical reorganization during early childhood. Brain and Cognition, 20: 24-50.

Thatcher, R.W. (1994). Psychopathology of Early Frontal Lobe Damage: Dependence on Cycles of Postnatal Development. Developmental Pathology, 6: 565-596.

Thatcher, R. W., Biver, C., McAlaster, R and Salazar, A.M. (1998). Biophysical linkage between MRI and EEG coherence in traumatic brain injury. NeuroImage, 8(4), 307-326.

Thatcher, R.W. (1998). A predator-prey model of human cerebral development. In: K. Newell and P. Molenaar Editors, Dynamical Systems in Development, L. Erlbaum Assoc, New Jersey.

Thatcher, R.W., North, N. and Biver, C.J. (2007). Development of cortical connections using EEG coherence and phase (submitted for publication).

Thompson, J.M.T. and Stewart, H.B. (1986). Nonlinear Dynamics and Chaos. John Wiley & Sons, New York.

Vaadia, E., Haalman, L., Abeles, M., Bergman, H., Prut, Y., Slovin, H. and Aertsen, A. (1995). Dynamics of neuronal interactions in monkey cortex in relation to behavior events. Nature, 373(6514): 515-518.

Varela, F.J. (1995). Resonant cell assemblies: a new approach to cognitive functions and neuronal synchrony. Biol. Res., 28(1): 81-95.

Varela, F.J., Lachaux, J.-P., Rodriguez, E., and Martinerie, J. (2001). The brainweb: phase synchronization and large-scale integration. Nat. Rev., Neurosci., 2(4): 229-239.

van Baal, G.C., Boomsma, D.I. and de Geus, E.J. (2001). Longitudinal genetic analysis of EEG coherence in young twins. Behav. Genet., 31(6):637-651.

Van Beijsterveldt, C.E., Molenaar, P.C., de Geus, E.J. and Boomsma, D.I. (1998). Genetic and environmental influences on EEG coherence. Behav. Genet., 28(6): 443-453.